

Multi-objective Deep Reinforcement Learning for Mobile Edge Computing

Ning Yang, Junrui Wen, Meng Zhang*, Ming Tang

Abstract—Mobile edge computing (MEC) is essential for next-generation mobile network applications that prioritize various performance metrics, including delays and energy consumption. However, conventional single-objective scheduling solutions cannot be directly applied to practical systems in which the preferences of these applications (i.e., the weights of different objectives) are often unknown or challenging to specify in advance. In this study, we address this issue by formulating a multi-objective offloading problem for MEC with multiple edges to minimize expected long-term energy consumption and transmission delay while considering unknown preferences as parameters. To address the challenge of unknown preferences, we design a multi-objective (deep) reinforcement learning (MORL)-based resource scheduling scheme with *proximal policy optimization* (PPO). In addition, we introduce a well-designed state encoding method for constructing features for multiple edges in MEC systems, a sophisticated reward function for accurately computing the utilities of delay and energy consumption. Simulation results demonstrate that our proposed MORL scheme enhances the hypervolume of the Pareto front by up to 233.1% compared to benchmarks. Our full framework is available at https://github.com/gracefulning/mec_morl_multipolicy.

Index Terms—Mobile edge computing, multi-objective reinforcement learning, resource scheduling.

I. INTRODUCTION

The rise of next-generation networks and the increasing use of mobile devices have resulted in an exponential growth of data transmission and diverse computing needs. With the emergence of new computing-intensive applications, there is a possibility that device computing capacity may not suffice. Cloud computing is one solution that can provide the necessary resources, but it may also result in latency issues.

To address this challenge, mobile edge computing (MEC) has emerged as a promising computing paradigm that offloads computing workload to edge or cloud networks and can achieve low latency and high efficiency [1]–[3].

In MEC systems, task offloading is crucial in achieving low latency and energy consumption [4]. By selectively offloading computing tasks to edge or cloud users based on their requirements, MEC systems can optimize resource utilization and improve performance. For example, edge servers may be effective for low-latency tasks that require real-time processing,

while cloud users may be more suitable for computationally intensive tasks. Additionally, other factors, such as edge load and transmission rate, need to be considered when designing offloading schemes. Task offloading schemes in MEC systems present two key challenges.

Challenge 1: The natural MEC network environments are full of dynamics and uncertainty.

The scheduling of offloading in MEC systems is challenging due to the dynamic and unpredictable nature of users' workloads and computing requirements. The presence of stochastic parameters in the problem poses challenges to the application of traditional optimization methods. Myopically optimizing the offloading decision of the current step is ineffective since it cannot account for long-term utilities.

The application of deep reinforcement learning (DRL) has shown substantial potential in addressing sequential decision-making problems and is an attractive technique for dynamic MEC environments [4], [5]. The existing works have demonstrated the effectiveness of applying DRL in MEC systems to address unknown dynamics. For instance, Cui et al. [6] employed DRL to solve the user association and offloading sub-problem in MEC networks. Lei et al. [7] investigated computation offloading and multi-user scheduling algorithms in edge IoT networks and proposed a DRL algorithm to solve the continuous-time problem, supporting implementation based on semi-distributed auctions. Jiang et al. [8] proposed an online DRL-based resource scheduling framework to minimize the delay in large-scale MEC systems. However, there is another challenge that requires consideration.

Challenge 2: Users who initiate tasks may have diverse preferences regarding delay and energy consumption.

In various mobile applications such as health care, transportation, and virtual reality, among others, delay in processing data can have serious consequences, particularly in emergency situations. However, in industrial and unmanned aerial networks, energy consumption is subject to strict limits, and thus, computing applications in these areas may prioritize energy over delay. Therefore, offloading scheduling in MEC systems requires a well-designed balance between delay and energy consumption. Moreover, one of the most critical considerations in designing an offloading scheme for MEC systems is that target applications may not be known in advance.

Regrettably, existing studies on MEC (e.g., [4], [6]–[10]), most of them have focused exclusively on single-objective methods. In practice, many scheduling problems in MEC systems are in nature *multi-objective*. Since these studies have not taken into account multi-objective methods, they cannot address

Ning Yang and Junrui Wen are with Institute of Automation, Chinese Academy of Sciences, Beijing, 100190, China. (e-mail: ning.yang@ia.ac.cn, yvwotogo@gmail.com).

Meng Zhang is with the ZJU-UIUC Institute, Zhejiang University, Zhejiang, 314499, China. (e-mail: mengzhang@intl.zju.edu.cn).

Ming Tang is with the Department of Computer Science and Engineering, Southern University of Science and Technology, Shenzhen, 518055, China. (e-mail: tangm3@sustech.edu.cn).

(*Corresponding author: Meng Zhang)

the second challenge of MEC systems, which is dealing with diverse and unknown preferences. The dynamic and uncertain nature of the environments, the diversity of preferences, and the computational infeasibility of classical methods motivate us to seek out new methodologies to address these issues.

Note that although some may argue that we can still directly apply single-objective DRL by simply taking a weighted sum (known as scalarization), this is, in fact, not true due to the following issues [11]:

- 1) *Impossibility*: Weights may be unknown when designing or learning an offloading scheme.
- 2) *Infeasibility*: Weights may be diverse, which is true when MEC systems have different restrictive constraints on latency or energy.
- 3) *Undesirability*: Even if weights are known, nonlinear objective functions may lead to non-stationary optimal policies.

To effectively address these challenges, we propose employing multi-objective reinforcement learning (MORL) to design a task offloading method. We summarize our main contributions as follows:

- *Multi-objective MEC Framework*: We formulate the multi-objective MDP (Markov decision process) problem framework. Compared with previous works, our framework focuses on the Pareto optimal solutions, which characterize the performance of the offloading scheduling policy with multiple objectives under different preferences.
- *Multi-objective Decision Model*: We propose a novel MORL method based on proximal policy optimization (PPO) to solve the multi-objective problem. Our proposed method aims to achieve the Pareto near-optimal solution for diverse preferences. Moreover, we introduce a well-designed encoding method to construct features for multi-edge systems and a sophisticated reward function to compute delay and energy consumption.
- *Numerical Results*: Compared to benchmarks, our MORL scheme increases the hypervolume of the Pareto front up to 233.1%.

II. SYSTEM MODEL

We consider a set of servers $\mathcal{E} = \{0, 1, 2, \dots, E\}$ with one remote cloud server (denoted by index 0) and E edge servers, and consider a set of users $\mathcal{U} = \{1, 2, \dots, U\}$ in a MEC system, as shown in Fig. 1. We use index $e \in \mathcal{E}$ to denote a server. Index $u \in \mathcal{U}$ denotes a user. Our model is a continuous-time system and has discrete decision steps. Consider one episode consisting of T steps, and each step is denoted by $t \in \{1, 2, \dots, T\}$, each with a duration of Δt seconds.

Multiple users request MEC services from servers. At the beginning of each step, the arrival time of a series of tasks follows a Poisson distribution for each user, and the Poisson arrival rate for each user is λ_p . The tasks are placed in a queue with a first in, first out (FIFO) queue strategy. In each step, the system will offload the first task in the queue to one of the servers. Then the task is removed from the queue. Let $\mathcal{M} = \{1, 2, \dots, M\}$ denote the set of tasks in an episode. We use

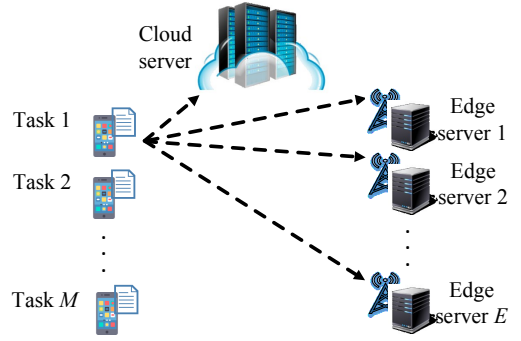


Fig. 1: An illustrative example system model of MEC.

$m \in \mathcal{M}$ to denote a task and use L_m to denote the size of task m , which follows an exponential distribution [12] with mean \bar{L} .

We consider a Rayleigh fading channel model in the MEC network. We denote $\mathbf{h} \in \mathbb{R}^{U \times (E+1)}$ as the $U \times (E+1)$ channel matrix. Thus, the achievable data rate from user u to server e is

$$C_{u,e} = W \log_2 \left(1 + \frac{p^{\text{off}} |h_{u,e}|^2}{\sigma^2} \right), \forall u \in \mathcal{U}, e \in \mathcal{E}, \quad (1)$$

where σ^2 is additive white Gaussian noise (AWGN) power, and W is the bandwidth. The offloading power is p^{off} , and the channel coefficient from user u to server e is $h_{u,e}$.

Offloading: We denote the offloading decision (matrix) as $\mathbf{x} = \{x_{m,e}\}_{m \in \mathcal{M}, e \in \mathcal{E}}$, where $x_{m,e} \in \{0, 1\}$ is an offloading indicator variable; $x_{m,e} = 1$ indicates that task m is offloaded to server e . If task m comes from user u . The offloading delay for task m is given by [13]

$$T_m^{\text{off}} = \sum_{e \in \mathcal{E}} x_{m,e} \frac{L_m}{C_{u,e}}, \quad \forall m \in \mathcal{M}. \quad (2)$$

The offloading energy consumption for task m with offloading power p^{off} is

$$E_m^{\text{off}} = p^{\text{off}} T_m^{\text{off}}, \quad \forall m \in \mathcal{M}. \quad (3)$$

Execution: Each server executes tasks in parallel. We denote the beginning of step t as time instant τ_t , given by $\tau_t = t\Delta t$. The computing speed for each task in server e at time instant τ_t is

$$q_e(\tau_t) = \frac{f_e}{n_e^{\text{exe}}(\tau_t)\eta}, \quad \forall e \in \mathcal{E}, \quad (4)$$

where f_e is the CPU frequency (in cycles per second) of server e , and η is the number of CPU cycles required for computing a one-bit task. We define $n_e^{\text{exe}}(\tau_t)$ as the number of tasks that are being executed in server e at time τ_t . The $n_e^{\text{exe}}(\tau_t)$ tasks share equally the computing resources of server e . Thus, we give the relation between task size L_m and execution delay T_m^{exe} for

task m as

$$\begin{aligned} L_m &= g_m(T_m^{\text{exe}}) \\ &= \sum_{e \in \mathcal{E}} x_{m,e} \int_{m\Delta t + T_m^{\text{off}}}^{m\Delta t + T_m^{\text{off}} + T_m^{\text{exe}}} q_e(\tau) d\tau, \forall m \in \mathcal{M}, \end{aligned} \quad (5)$$

where τ is a time instant. The integral function $g_m(T_m^{\text{exe}})$ denotes the aggregate executed size for task m from $m\Delta t + T_m^{\text{off}}$ to $m\Delta t + T_m^{\text{off}} + T_m^{\text{exe}}$. Therefore, execution time delay T_m^{exe} of task m is

$$T_m^{\text{exe}} = g_m^{-1}(L_m), \forall m \in \mathcal{M}. \quad (6)$$

The total energy consumption of execution for task m is given by [13]

$$E_m^{\text{exe}} = \sum_{e \in \mathcal{E}} x_{m,e} \kappa \eta f_e^2 L_m, \forall m \in \mathcal{M}, \quad (7)$$

where κ denotes an effective capacitance coefficient for each CPU cycle.

To summarize, the overall delay and the overall energy consumption for task $m \in \mathcal{M}$ are

$$T_m = T_m^{\text{off}} + T_m^{\text{exe}}, E_m = E_m^{\text{off}} + E_m^{\text{exe}}, \quad (8)$$

respectively.

The mean of task size \bar{L} represents the demand for tasks. If the computational capability of the system exceeds the demand, the scheduling pressure decreases. Conversely, if the demand surpasses the capability, the system will continuously accumulate tasks over time. Therefore, we consider a system that balances computational capability and task demand. The mean of task size \bar{L} satisfies

$$\Delta t \left(\sum_{e \in \mathcal{E}} \frac{f_e}{\eta} \right) = \lambda_p \bar{L} U, \quad (9)$$

A. Problem Formulation

Based on different application scenarios, MEC networks have diverse preferences over energy consumption and delay. Therefore, we aim to design a scheduling policy to achieve the Pareto optimal solution between energy consumption and delay. We cannot directly apply single-objective DRL by simply taking a weighted sum due to impossibility (i.e., weights may be unknown), infeasibility (i.e., MEC systems have different restrictive constraints on latency or energy), and undesirability (i.e., non-stationary optimal policies). This motivates us to use MORL to achieve Pareto optimal solution for any potential preference. We introduce the preference vector $\omega = (\omega_T, \omega_E)$ to weight delay and energy consumption, which satisfies $\omega_T + \omega_E = 1$. The subscript T denotes delay about, while the subscript E denotes energy consumption about in our study.

A (stochastic) policy is a mapping $\pi : \mathcal{S} \times \mathcal{A} \rightarrow [0, 1]$, where \mathcal{S} is the state space of the system and \mathcal{A} is the offloading action space, we will formally define them in next section. For any given task m and system state, policy π selects an offloading decision $x_{m,e}$ according to a certain probability distribution. Given any one possible ω , the multi-objective

resource scheduling problem under the policy π is given by

$$\min_{\pi} \mathbb{E}_{\mathbf{x} \sim \pi} \left[\sum_{m \in \mathcal{M}} \gamma^m (\omega_T T_m + \omega_E E_m) \right] \quad (10a)$$

$$\text{s.t. } x_{m,e} \in \{0, 1\}, \forall m \in \mathcal{M}, \forall e \in \mathcal{E}, \quad (10b)$$

$$\sum_{e \in \mathcal{E}} x_{m,e} \leq 1, \forall m \in \mathcal{M}, \quad (10c)$$

where constraint (10b) restricts task offloading variables to be binary, and constraint (10c) guarantees that each task can be only offloaded to one server. A discount factor γ characterizes the discounted objective in the future. The expectation \mathbb{E} accounts for the distribution of the task size L_m , the arrival of users, and stochastic policy π .

B. Multi-objective Metrics

To facilitate multi-objective analysis, we further introduce the following notions. Consider a preference set $\Omega = \{\omega_1, \omega_2, \dots, \omega_n\}$ with n preferences. A scheduling policy set $\Pi = [\pi_1, \pi_2, \dots, \pi_n]$ with n policies solving problem (10a) given corresponding preferences in Ω . Let \mathbf{y} denote the performance, given by

$$\mathbf{y} = \{y_T, y_E\} = \left\{ \sum_{m \in \mathcal{M}} T_m, \sum_{m \in \mathcal{M}} E_m \right\}. \quad (11)$$

A performance of Π is denoted as $\mathbf{Y} = \{\mathbf{y}^{\pi_1}, \mathbf{y}^{\pi_2}, \dots, \mathbf{y}^{\pi_n}\}$. We consider the following definition to characterize the optimal trade-offs between two performance metrics:

Definition 1 (Pareto front [11]): For a policy set Π , Pareto front $PF(\Pi)$ is the undominated set :

$$PF(\Pi) = \{\pi \in \Pi \mid \nexists \pi' \in \Pi : \mathbf{y}^{\pi'} \succ_P \mathbf{y}^{\pi}\}, \quad (12)$$

where \succ_P is the Pareto dominance relation, satisfying

$$\begin{aligned} \mathbf{y}^{\pi} \succ_P \mathbf{y}^{\pi'} &\iff \\ (\forall i : y_i^{\pi} \geq y_i^{\pi'}) \wedge (\exists i : y_i^{\pi} > y_i^{\pi'}), i \in \{T, E\}. \end{aligned} \quad (13)$$

We aim to approximate the exact Pareto front [11] by searching for policies set Π . The following hypervolume metric can measure the quality of an approximation:

Definition 2 (Hypervolume metric [14]): In the multi-objective MEC scheduling problem, as a Pareto front approximation $PF(\Pi)$, the hypervolume metric is

$$\mathcal{V}(PF(\Pi)) = \int_{\mathbb{R}^2} \mathbb{I}_{V_h(PF(\Pi))}(z) dz, \quad (14)$$

where $V_h(PF(\Pi)) = \{z \in Z \mid \exists \pi \in PF(\Pi) : \mathbf{y}^{\pi} \succ_P z \succ_P \mathbf{y}^{\text{ref}}\}$, and $\mathbf{y}^{\text{ref}} \in \mathbb{R}^2$ is a reference performance point. Function $\mathbb{I}_{V_h(PF(\Pi))}$ is an indicator function that returns 1 if $z \in V_h(PF(\Pi))$ and 0 otherwise.

The multi-objective resource scheduling problem is still a challenge for MEC networks for the following reasons:

- The natural MEC network environments are full of dynamics and uncertainty, leading to unknown preferences of MEC systems.
- The computation complexity of the conventional optimization method is demanding since the goal is to get a vector

reward instead of a reward value. The objective function (10a) and the feasible set of constraints (10b) and (10c) are non-convex due to binary variables \mathbf{x} .

The aforementioned problems motivate us to design a MORL scheme to solve (10).

III. MORL SCHEDULING SOLUTION

This section considers the situation of multiple preferences. We consider that a (central) agent makes all offloading decisions in a fully-observable setting. We model the MEC environment as a MOMDP framework. In the subsection, we first introduce the MOMDP framework, which includes a well-designed state encoding method and a sophisticated reward function. Then, we present our algorithm by introducing aspects including the neural network architecture and policy update method.

A. The MOMDP Framework

Definition 3 (MOMDP [11]): A MOMDP is a tuple $\langle \mathcal{S}, \mathcal{A}, \mathcal{T}, \gamma, \mu, \mathcal{R} \rangle$ that contains state space \mathcal{S} , action space \mathcal{A} , probabilistic transition process $\mathcal{T} : \mathcal{S} \times \mathcal{A} \rightarrow \mathcal{S}$, discount factor $\gamma \in [0, 1)$, a probability distribution over initial states $\mu : \mathcal{S} \rightarrow [0, 1]$, and a vector-valued reward function $\mathcal{R} : \mathcal{S} \times \mathcal{A} \rightarrow \mathbb{R}^2$ that specifies the immediate reward for the delay objective and the energy consumption objective.

For a decision step t , an agent offloads task m from user u . It has $m = t$ for task index m and step-index t . We specify the MOMDP framework in the following:

State \mathcal{S} : We consider $E + 1$ servers (E edge servers and a cloud server). Hence, the state $\mathbf{s}_t \in \mathcal{S}$ at step t is a fixed length set and contains $E + 1$ server information vectors. We formulate state \mathbf{s}_t as $\mathbf{s}_t = \{\mathbf{s}_{t,e} | e \in \mathcal{E}\}$. The information vector of server e at step t is

$$\mathbf{s}_{t,e} = (L_m, C_{u,e}, f_e, n_e^{\text{exe}}(\tau_t), E, \mathcal{B}_e), \quad \forall e \in \mathcal{E}. \quad (15)$$

State $\mathbf{s}_{t,e}$ contains task size L_m , data rate $C_{u,e}$, CPU frequency f_e , the number of execution task $n_e^{\text{exe}}(\tau_t)$, the number of edge server E , and task histogram vector \mathcal{B}_e , which is the residual size distribution for tasks executed in server e at time instant τ_t . That is,

$$\mathcal{B}_e(\tau_t) = (b_{1,e}^{\text{exe}}(\tau_t), b_{2,e}^{\text{exe}}(\tau_t), \dots, b_{N,e}^{\text{exe}}(\tau_t)). \quad (16)$$

Histogram vector \mathcal{B}_e has N bins. We denote one of previous tasks as m' and denote the execution residual size of task m' at time instant τ_t as $L_{m'}^{\text{res}}(\tau_t)$. In Eq. (16), the i -th value $b_{i,e}^{\text{exe}}(\tau_t)$ in \mathcal{B}_e denotes the number of tasks with execution residual size $L_{m'}^{\text{res}}(\tau_t)$ within the range of $[i-1, i)$ Mbits. Specifically, the last element $b_{N,e}^{\text{exe}}(\tau_t)$ denotes the number of tasks with execution residual size $L_{m'}^{\text{res}}(\tau_t)$ within the range of $[N-1, +\infty)$ Mbits. The execution residual size $L_{m'}^{\text{res}}(\tau_t)$ is given by

$$L_{m'}^{\text{res}}(\tau_t) = L_{m'} - \min(g_{m'}((\tau_t - m' \Delta t), L_{m'}), \forall \tau_t \in [t \Delta t, T \Delta t], m' \in \{1, 2, \dots, m-1\}). \quad (17)$$

Action \mathcal{A} : The action $a_t \in \mathcal{A}$ denotes that offloading task m to which server. The action space is $\mathcal{A} = \{0, 1, 2, \dots, E\}$. Hence, the action at step t is represented by the following

$$a_t = \sum_{e \in \mathcal{E}} ex_{m,e}(t). \quad (18)$$

Transition \mathcal{T} : It describes the transition from \mathbf{s}_t to \mathbf{s}_{t+1} with action a_t , which is denoted by $P(\mathbf{s}_{t+1} | \mathbf{s}_t, a_t)$.

Reward \mathcal{R} : Unlike a classical MDP setting in which each reward is a scalar, a multi-objective setting requires a vector. Therefore, our reward (profile) function is given by $\mathcal{R} : \mathcal{S} \times \mathcal{A} \rightarrow \mathbb{R}^2$. We denote the reward of energy consumption and delay as r_E and r_T . If the agent offloads task m to server e at step t , the reward of energy consumption for state \mathbf{s}_t and action a_t is

$$r_E(\mathbf{s}_t, a_t) = -\hat{E}_m, \quad (19)$$

where \hat{E}_m is the estimated energy consumption of task m . Through (8), we can compute the energy consumption of task m . The MORL algorithm maximizes the reward, which is thus the negative of energy consumption. For one episode, the total reward for energy consumption is given by

$$R_E = \sum_{t=1}^T r_E(\mathbf{s}_t, a_t) = - \sum_{m \in \mathcal{M}} \hat{E}_m. \quad (20)$$

The reward for the delay is

$$r_T(\mathbf{s}_t, a_t) = - \left(\hat{T}_m + \sum_{m' \in \mathcal{M}_e(\tau_t)} \Delta \hat{T}_{m'}^{a_t} \right), \quad (21)$$

where \hat{T}_m is the estimated delay for task m , and $\mathcal{M}_e(\tau_t)$ is a set of tasks, which are executed in server e at time instant τ_t . The estimated correction of delay $\Delta \hat{T}_{m'}^{a_t}$ describes how much delay will increase to task m' with action a_t . For one episode, the total reward of delay has

$$R_T = \sum_{t=1}^T r_T(\mathbf{s}_t, a_t) = - \sum_{m \in \mathcal{M}} T_m. \quad (22)$$

To compute reward r_T , we rewrite Eq.(21) as

$$r_T(\mathbf{s}_t, a_t) = -\hat{T}_m - \sum_{m' \in \mathcal{M}_e(\tau_t)} (\hat{T}_{m'}^{a_t} - \hat{T}_{m'}^{a^*(t)}), \quad (23)$$

where $\hat{T}_{m'}^{a_t}$ denotes the estimated residual delay of task m' with taking action a_t at step t . The residual delay of task m' without taking action a_t is $\hat{T}_{m'}^{a^*(t)}$, which is the estimated residual delay at the end of step $t-1$. Next, we introduce the computation of the two cases.

(1) *The case without taking action a_t :* For task set $\mathcal{M}_e(\tau_t)$ with $n_e^{\text{exe}}(\tau_t)$ tasks, the execution residual size is a set $\mathcal{L}_{\mathcal{M}_e(\tau_t)}^{\text{res}} = \{L_{m'}^{\text{res}}(\tau_t) | m' \in \mathcal{M}_e(\tau_t)\}$. We sort residual task size set $\mathcal{L}_{\mathcal{M}_e(\tau_t)}^{\text{res}}$ in the ascending order and get a vector $\mathbf{L}_{\mathcal{M}_e(\tau_t)}^{\text{sort}} = (L_{1,e}^{\text{sort}}(\tau_t), L_{2,e}^{\text{sort}}(\tau_t), \dots, L_{n_e^{\text{exe}}(\tau_t),e}^{\text{sort}}(\tau_t))$, where $L_{i,e}^{\text{sort}}(\tau_t)$ is the i -th least residual task size in $\mathcal{L}_{\mathcal{M}_e(\tau_t)}^{\text{res}}$. Specifically, we define

$L_{0,e}^{\text{sort}}(\tau_t) = 0$. Then, we have

$$\begin{aligned} \sum_{m' \in \mathcal{M}_e(\tau_t)} \hat{T}_{m'}^{a^*(t)} &= \sum_{i=1}^{n_e^{\text{exe}}(\tau_t)} (n_e^{\text{exe}}(\tau_t) - i + 1) \hat{T}_{i,e}^{\text{dur}} \\ &= \sum_{i=1}^{n_e^{\text{exe}}(\tau_t)} \frac{\eta}{f_e} (n_e^{\text{exe}}(\tau_t) - i + 1)^2 (L_{i,e}^{\text{sort}}(\tau_t) - L_{i-1,e}^{\text{sort}}(\tau_t)), \end{aligned} \quad (24)$$

where $\hat{T}_{i,e}^{\text{dur}}$ denotes the estimated duration of time from the completing instant of residual task $L_{i-1,e}^{\text{sort}}(\tau_t)$ to the completing instant of residual task $L_{i,e}^{\text{sort}}(\tau_t)$.

(2) *The case with action a_t* : The MEC system completes offloading task m at time instant $\tau'_t = \tau_t + T_m^{\text{off}}$. We consider a high-speed communication system that offloading delay T_m^{off} is short than the duration of one step Δt and satisfies $T_m^{\text{off}} < \Delta t$. For task set $\mathcal{M}_e(\tau'_t)$ with $n_e^{\text{exe}}(\tau'_t)$ tasks, the execution residual size is a set $\mathcal{L}_{\mathcal{M}_e(\tau'_t)}^{\text{res}} = \{L_m^{\text{res}}(\tau'_t) | m \in \mathcal{M}_e(\tau'_t)\}$. We sort set $\mathcal{L}_{\mathcal{M}_e(\tau'_t)}^{\text{res}}$ in the ascending order and get a vector $\mathbf{L}_{\mathcal{M}_e(\tau'_t)}^{\text{sort}} = (L_{1,e}^{\text{sort}}(\tau'_t), L_{2,e}^{\text{sort}}(\tau'_t), \dots, L_{n_e^{\text{exe}}(\tau'_t),e}^{\text{sort}}(\tau'_t))$, where $L_{i,e}^{\text{sort}}(\tau'_t)$ is the i -th least residual task size in $\mathcal{L}_{\mathcal{M}_e(\tau'_t)}^{\text{res}}$. Then, it satisfies

$$\begin{aligned} \hat{T}_m + \sum_{m' \in \mathcal{M}_e(\tau'_t)} \hat{T}_{m'}^{a_t} \\ &= \sum_{i=1}^{n_e^{\text{exe}}(\tau_t)} (n_e^{\text{exe}} - i + 1) \min \left(\hat{T}_{i,e}^{\text{dur}}, \max \left(\hat{T}_m^{\text{off}} - \sum_{j=1}^{i-1} \hat{T}_{j,e}^{\text{dur}}, 0 \right) \right) \\ &\quad + \sum_{i=1}^{n_e^{\text{exe}}(\tau'_t)} \frac{\eta}{f_e} (n_e^{\text{exe}}(\tau'_t) - i + 1)^2 (L_{i,e}^{\text{sort}}(\tau'_t) - L_{i-1,e}^{\text{sort}}(\tau'_t)) + \hat{T}_m^{\text{off}}, \end{aligned} \quad (25)$$

where \hat{T}_m^{off} is the estimated offloading delay for task m with Eq.(2). In Eq.(25), the first term to the right of the equation estimates the sum of delay for tasks $\mathcal{M}_e(\tau_t)$ from time instant τ_t to τ'_t . The second term to the right of Eq.(25) estimates the sum of delay for tasks $\mathcal{M}_e(\tau'_t)$ from time instant τ'_t to infinity. The expression $\frac{\eta}{f_e} (L_{i,e}^{\text{sort}}(\tau'_t) - L_{i-1,e}^{\text{sort}}(\tau'_t))$ in Eq. (25) represents the required time from completing residual size $L_{i-1,e}^{\text{sort}}(\tau'_t)$ to completing residual size $L_{i,e}^{\text{sort}}(\tau'_t)$. To simplify the calculation of $L_{1,e}^{\text{sort}}(\tau'_t) - L_{0,e}^{\text{sort}}(\tau'_t)$, we define $L_{0,e}^{\text{sort}}(\tau'_t) = 0$ specifically.

To summarize, if the agent offloads task m to server e at step t , the reward of delay is

$$\begin{aligned} r_T(\mathbf{s}_t, a_t) &= -\hat{T}_m^{\text{off}} + \sum_{i=1}^{n_e^{\text{exe}}(\tau_t)} (n_e^{\text{exe}}(\tau_t) - i + 1) \hat{T}_{i,e}^{\text{dur}} \\ &\quad - \sum_{i=1}^{n_e^{\text{exe}}(\tau_t)} (n_e^{\text{exe}} - i + 1) \min \left(\hat{T}_{i,e}^{\text{dur}}, \max \left(\hat{T}_m^{\text{off}} - \sum_{j=1}^{i-1} \hat{T}_{j,e}^{\text{dur}}, 0 \right) \right) \\ &\quad - \sum_{i=1}^{n_e^{\text{exe}}(\tau'_t)} \frac{\eta}{f_e} (n_e^{\text{exe}}(\tau'_t) - i + 1)^2 (L_{i,e}^{\text{sort}}(\tau'_t) - L_{i-1,e}^{\text{sort}}(\tau'_t)). \end{aligned} \quad (26)$$

To achieve the MORL algorithm, we compute a scalarized

reward given preference ω :

$$r_\omega(\mathbf{s}_t, a_t) = \omega^T \times (\alpha_T r_T(\mathbf{s}_t, a_t), \alpha_E r_E(\mathbf{s}_t, a_t)), \quad (27)$$

where α_T and α_E are coefficients for adjusting delay $r_T(t)$ and energy consumption $r_E(t)$ to the same order of magnitude. The total reward of one episode is

$$R_\omega = \sum_{t=1}^T r_\omega(\mathbf{s}_t, a_t). \quad (28)$$

B. MORL Scheduling

We train DRL-based scheduling policies based on a PPO algorithm [15], which is a family of policy gradient (PG) methods. The PPO algorithm can sample the data from the transition several times instead of one time within each episode. It improves the sampling efficiency than traditional PG methods. The neural networks with parameters θ contain an actor network and a critic network. In the training phase, the MORL algorithm trains a parametric network for each preference. In the evaluation phase, the parametric network evaluates the Pareto front of energy consumption and delay for multi-edge servers in the MEC environment.

We use generalized advantage estimator (GAE) technology to reduce the variance of policy gradient estimates [16]. The GAE advantage function for objective $i \in \{T, E\}$ is

$$\hat{A}_i(t) = \sum_{t'=t}^{T-1} \gamma \lambda (\alpha_i r_i(\mathbf{s}_{t'}, a_{t'}) + \gamma V_{i,\theta}(\mathbf{s}_{t'+1}) - V_{i,\theta}(\mathbf{s}_{t'})), \quad (29)$$

where λ is a GAE discount factor within $[0, 1]$, and $V_{i,\theta}(\mathbf{s}(t))$ denotes the value of state $\mathbf{s}(t)$. Value function $V_{i,\theta}(\cdot)$ is estimated by a critic network.

In the PPO algorithm, the gradient direction of objective $i \in \{T, E\}$ is given as

$$\begin{aligned} \nabla_{\theta} L_i^{\text{clip}}(\theta) &= \mathbb{E}_t [\min (r_t^{\text{pr}}(\theta), \text{clip}(r_t^{\text{pr}}(\theta), 1 - \epsilon, 1 + \epsilon)) \\ &\quad \hat{A}_i(t) \nabla \log \pi_{\theta}(a_t | \mathbf{s}_t)], \end{aligned} \quad (30)$$

where ϵ is a clip hyperparameter. The probability ratio is $r_t^{\text{pr}}(\theta) = \frac{\pi_{\theta}(a_t | \mathbf{s}_t)}{\pi_{\theta_{\text{old}}}(a_t | \mathbf{s}_t)}$. The surrogate objective is $r_t^{\text{pr}}(\theta) \hat{A}_t$, which corresponds to a conservative policy iteration. The objective is constrained by $\text{clip}(r_t^{\text{pr}}(\theta) \hat{A}_t, 1 - \epsilon, 1 + \epsilon)$, to penalize the policy move outside interval $[1 - \epsilon, 1 + \epsilon]$.

Given the gradient directions of the two objectives, a policy can reach the Pareto front by following a direction in ascent simplex [17]. An ascent simplex is defined by the convex combination of single-objective gradients. As shown in Fig. 2, the green arrow and blue arrow denote the gradient directions of the delay objective and energy consumption objective, respectively. The light blue area stands for an ascent simplex.

For reward function $r_\omega(\cdot)$, the gradient direction of preference ω is

$$\begin{aligned} \nabla_{\theta} L_{\omega}^{\text{clip}}(\theta) &= \mathbb{E}_t [\min (r_t^{\text{pr}}(\theta), \text{clip}(r_t^{\text{pr}}(\theta), 1 - \epsilon, 1 + \epsilon)) \\ &\quad \omega^T (\hat{A}_1(t), \hat{A}_2(t)) \nabla \log \pi_{\theta}(a_t | \mathbf{s}_t)] \\ &= \omega^T (\nabla_{\theta} L_1^{\text{clip}}(\theta), \nabla_{\theta} L_2^{\text{clip}}(\theta)). \end{aligned} \quad (31)$$

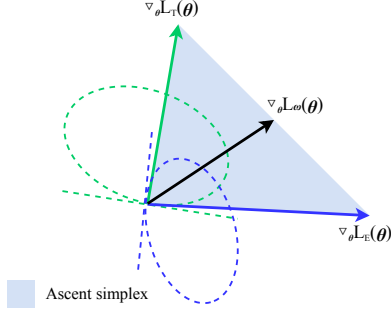


Fig. 2: The ascent simplex in a 2-objectives problem.

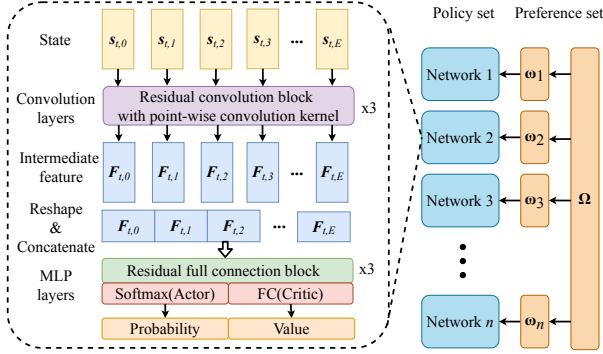


Fig. 3: The neural network framework of a scheduling policy.

The vector $\nabla_{\theta} L_{\omega}^{clip}(\theta)$ is a gradient direction in ascent simplex. It makes a policy to the Pareto front by optimizing neural network parameters θ .

As an example shown in Fig. 3, a neural network contains convolution layers and multi-layer perceptron (MLP) layers. The convolution layers encode the input state with point-wise convolution kernel and turn information vector s_t of each server to feature vector F . We reshape all feature vectors and concatenate them to get the total feature vector. The MLP layers encode the total feature vector to get the output. For an actor-network, the output is probability $\pi_{\theta}(a_t|s_t)$ of each action. For a critic network, the output is estimated value $\omega^T[V_{T,\theta}(s_t), V_{E,\theta}(s_t)]$ for preference ω . Additionally, we apply deep residual learning technology [18] to build the neural network architecture to address the problem of vanishing/exploding gradients.

We present the proposed MORL algorithm in Algorithm 1. For each preference ω in set Ω , we train a policy with PPO method to maximize reward R_{ω} and approximate Pareto front $PF(\Pi)$. To improve the training efficiency achieved by [19], we reuse trained neural network parameters θ_{ω_i} ($i \in \{1, 2, \dots, n-1\}$) to initialize the next parameters $\theta_{\omega_{i+1}}$, with a similar preference.

IV. SIMULATION RESULTS

In this section, we evaluate the performances of the MORL scheduling scheme and compare it with benchmarks. We introduce the simulation setup and evaluation metrics. Then, we analyze the Pareto fronts and compare them with the benchmarks.

Algorithm 1 MORL-based Scheduling

- 1: Initialize replay memory buffer D_{ω} , policy parameters θ_{ω} for each preference ω
- 2: Initialize the learning rate α and the number of episodes T^{epi} for training.
- 3: Set policies set $\Pi \leftarrow \emptyset$
- 4: **for** each preference ω **do**
- 5: **for** each episode T^{epi} **do**
- 6: **for** each step t **do**
- 7: $a_t \sim \pi_{\theta_{\omega}}(s_t)$
- 8: $s_{t+1} \sim \mathcal{T}(s_{t+1}|s_t)$
- 9: $D_{\omega} = D_{\omega} \cup \{(s_t, a_t, r_{\omega}(s_t, a_t), s_{t+1})\}$
- 10: **end for**
- 11: $\theta_{\omega} \leftarrow \theta_{\omega} + \alpha \nabla_{\theta_{\omega}} L_{\omega}^{clip}(\theta_{\omega})$
- 12: **end for**
- 13: $\Pi \leftarrow \Pi \cup \pi_{\theta_{\omega}}$
- 14: **end for**
- 15: Compute Pareto front $PF(\Pi)$

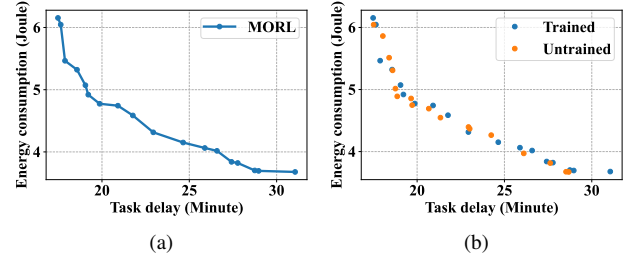


Fig. 4: The Pareto front of the MORL scheme.

A. Simulation Setup

We set the preference set as Ω with an equal interval 0.02 and obtain 50 preferences to fit the Pareto front. Each preference's performance contains total delay and energy consumption for all tasks in one episode. We evaluate a performance (delay or energy consumption) with an average of 1000 episodes. Furthermore, we analyze the Pareto front of the proposed scheme and compare it with benchmarks. A disk coverage has a radius of 1000m to 2000m for a cloud server and 50m to 500m for an edge server. Each episode needs to initial different radiuses for the cloud and edge servers. We set the mean of task size \bar{L} according to Eq. (9).

B. Evaluation Metrics

We consider the following metrics to evaluate the performances of the proposed algorithms.

- **Energy Consumption:** The total energy consumption of one episode given as $\sum_{m=1}^M E_m^{off} + E_m^{exe}$, and average energy consumption per Mbits task of one episode given by $\sum_{m=1}^M \frac{E_m^{off} + E_m^{exe}}{ML}$.

TABLE I: Model Parameters

Resource Scheduling Hyperparameters	Values
The number of steps for one episode T	100
Step duration Δt	1 s
The number of users U	10
The number of tasks M	100
System bandwidth W	16.6MHz [20]
Offloading power p^{off}	10 mW
The number of CPU cycles η for one-bit task	10^3
Effective capacitance coefficient κ	5×10^{-31}
CPU frequency of cloud server f_0	4.0 GHz
CPU frequency of edge server f_e	2.0 GHz
Poisson arrival rate λ_p for each user	0.1
DRL Hyperparameters	Values
The episodes for training T^{epi}	1.92×10^6
Replay memory	1×10^5
Batch size	4096
Learning rate	1×10^{-6}
Discount factor γ	0.9
GAE discount factor λ	0.95
Clip parameter ϵ	0.2

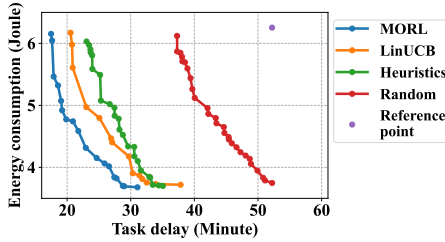


Fig. 5: The Pareto fronts of MORL scheme and other schemes.

- **Task Delay:** The total task delay given as $\sum_{m=1}^M T_m^{\text{off}} + T_m^{\text{exe}}$ and average delay per Mbits task of one episode given by $\sum_{m=1}^M \frac{T_m^{\text{off}} + T_m^{\text{exe}}}{ML}$.
- **Pareto Front:** $PF(\Pi) = \{\pi \in \Pi \mid \nexists \pi' \in \Pi : \mathbf{y}^{\pi'} \succ_P \mathbf{y}^{\pi}\}$, where the symbols are defined by Eq. (12).
- **Hypervolume metric:** $\mathcal{V}(PF(\Pi)) = \int_{\mathbb{R}^2} \mathbb{1}_{V_h(PF(\Pi))}(z) dz$, where the symbols are defined by Eq. (14).

C. Simulation results

1) *Pareto Front Analysis:* Fig. 4a presents the Pareto front of the proposed MORL scheme. In this scenario, the number of

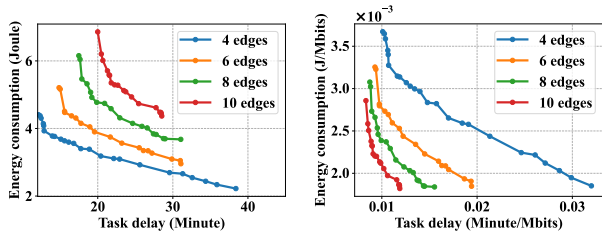
edge servers is $E = 8$, and the mean of task size $\bar{L} = 20$ Mbits. The Pareto front shows that minimizing the delay (the leftmost point) increases energy by 67.3%, but minimizing energy (the rightmost point) increases the delay by 77.6%. Fig. 4b shows the points of the Pareto front with trained and untrained preferences. Each untrained preference lies intermediate to the adjacent trained preferences. The result shows that by reusing trained parameters to the most similar preference, our MORL scheme has generalization for new preferences.

2) *Performance Comparison with Benchmarks:* We evaluate the performance of the proposed MORL algorithms and compare it with a linear upper confidence bound (LinUCB)-based scheme [21], a heuristics-based scheme, and a random-based scheme. LinUCB algorithms belong to contextual multi-arm bandit (MAB) algorithms, widely used in task offloading problems [22], [23]. Some work [24], [25] apply heuristic methods to schedule for offloading.

- *LinUCB-based scheme:* Offloading scheme based on a kind of contextual MAB algorithm. This scheme uses states as MAB contexts and learns a policy by exploring different actions.
- *Heuristics-based scheme:* Heuristic methods greedily select the server with the optimal weighted sum of estimated running speed and energy consumption for the current step.
- *Random-based scheme:* The agent offloads a task to a cloud server or a random edge server according to probability. We adjust the probability to compute a Pareto front.

Fig. 5 illustrates the Pareto front comparison of the proposed MORL scheme with other schemes. In this scenario, the system has $E = 8$ and $\bar{L} = 20$ Mbits. We select the position which denotes the maximum delay and energy consumption of the performance profiles in Fig. 5 as the reference point to compute the hypervolumes. The hypervolume of the proposed MORL scheme is 80.7, the LinUCB-based scheme is 69.9, the heuristics-based scheme is 63.9, and a random-based scheme is 24.2. Compared with a LinUCB-based scheme and a random-based scheme, the proposed MORL scheme increases the hypervolume of the Pareto front by $\frac{80.7-69.9}{69.9} = 15.5\%$ and $\frac{80.7-24.2}{24.2} = 233.1\%$. As shown, the proposed MORL scheme significantly outperforms other schemes. The MORL scheme has dynamic adaptability to learn the dynamics of task arrival and server load, which enables it to achieve better scheduling.

3) *Pareto Front Analysis in Multi-edge Scenarios:* We evaluate the Pareto front of the proposed MORL algorithm in scenarios with different edge server quantities. Fig. 6a illustrates the Pareto fronts of the proposed MORL algorithm in the case of edge quantity $E \in \{4, 6, 8, 10\}$. The mean of task size, represented by \bar{L} , is determined by Eq. (9) to balance the supply and demand of computational capability. The result shows that, in the balance case, the Pareto front of fewer edge servers and less demand case can dominate the more one. It means that while more edge servers may increase computational capability, matching them with more task demands may result in increased total energy consumption and task delay. The performances are computed per 1 Mbits task in Fig. 6b for a fair comparison.



(a) Pareto fronts of total delay and energy consumption (b) Pareto fronts of total delay and energy consumption per Mbits task

Fig. 6: Pareto fronts of the proposed MORL algorithm.

As the number of edge servers increases, the Pareto front of a more edge servers case can dominate the less one. The result shows that though more edge servers match more task demands, deploying more edge servers can significantly improve delay and energy consumption per Mbits tasks for each preference.

V. CONCLUSION

In this work, we investigated the offloading problem in MEC systems and proposed a MORL-based algorithm that can achieve Pareto fronts. A key advantage of the proposed MORL method is that it employs a MORL framework to offload tasks adopting various preferences, even untrained preferences.

We present a novel MOMDP framework for the multi-objective offloading problem in MEC systems. Our framework includes two key components: (1) a well-designed encoding method to construct features of multi-edge MEC systems. (2) a sophisticated reward function to evaluate the immediate utility of delay and energy consumption. Simulation results demonstrate the effectiveness of our proposed MORL scheme, which achieves Pareto fronts in various scenarios and outperforms benchmarks by up to 233.1%.

ACKNOWLEDGMENTS

The research leading to these results received funding from “Research on Combinatorial Optimization Problem Based on Reinforcement Learning” supported by Beijing Municipal Natural Science Foundation under Grant Agreement Grant No. 4224092. This work was supported in part by the National Natural Science Foundation of China under Grants 62202427 and Grants 62202214. In addition, it received funding from National Key R&D Program of China (2022ZD0116402).

REFERENCES

- [1] P. Mach and Z. Becvar, “Mobile edge computing: A survey on architecture and computation offloading,” *IEEE Communications Surveys & Tutorials*, vol. 19, no. 3, pp. 1628–1656, 2017.
- [2] Y. Mao, J. Zhang, and K. B. Letaief, “Dynamic computation offloading for mobile-edge computing with energy harvesting devices,” *IEEE Journal on Selected Areas in Communications*, vol. 34, no. 12, pp. 3590–3605, 2016.
- [3] C. You, K. Huang, H. Chae, and B.-H. Kim, “Energy-efficient resource allocation for mobile-edge computation offloading,” *IEEE Transactions on Wireless Communications*, vol. 16, no. 3, pp. 1397–1411, 2016.
- [4] J. Li, H. Gao, T. Lv, and Y. Lu, “Deep reinforcement learning based computation offloading and resource allocation for mec,” in *2018 IEEE Wireless Communications and Networking Conference (WCNC)*. IEEE, 2018, pp. 1–6.
- [5] V. Mnih, K. Kavukcuoglu, D. Silver, A. Graves, I. Antonoglou, D. Wierstra, and M. Riedmiller, “Playing atari with deep reinforcement learning,” *arXiv preprint arXiv:1312.5602*, 2013.
- [6] G. Cui, X. Li, L. Xu, and W. Wang, “Latency and energy optimization for mec enhanced sat-iot networks,” *IEEE Access*, vol. 8, pp. 55 915–55 926, 2020.
- [7] L. Lei, H. Xu, X. Xiong, K. Zheng, W. Xiang, and X. Wang, “Multiuser resource control with deep reinforcement learning in iot edge computing,” *IEEE Internet of Things J.*, vol. 6, no. 6, pp. 10 119–10 133, 2019.
- [8] F. Jiang, K. Wang, L. Dong, C. Pan, and K. Yang, “Stacked autoencoder-based deep reinforcement learning for online resource scheduling in large-scale mec networks,” *IEEE Internet of Things J.*, vol. 7, no. 10, pp. 9278–9290, 2020.
- [9] N. Yang, H. Zhang, and R. Berry, “Partially observable multi-agent deep reinforcement learning for cognitive resource management,” in *GLOBECOM 2020-2020 IEEE Global Communications Conference*. IEEE, 2020, pp. 1–6.
- [10] H. Zhang, N. Yang, W. Huangfu, K. Long, and V. C. Leung, “Power control based on deep reinforcement learning for spectrum sharing,” *IEEE Transactions on Wireless Communications*, vol. 19, no. 6, pp. 4209–4219, 2020.
- [11] D. M. Roijers, P. Vamplew, S. Whiteson, and R. Dazeley, “A survey of multi-objective sequential decision-making,” *Journal of Artificial Intelligence Research*, vol. 48, pp. 67–113, 2013.
- [12] L. Lei, H. Xu, X. Xiong, K. Zheng, and W. Xiang, “Joint computation offloading and multiuser scheduling using approximate dynamic programming in nb-iot edge computing system,” *IEEE Internet of Things J.*, vol. 6, no. 3, pp. 5345–5362, 2019.
- [13] K. Wang, F. Fang, D. Costa, and Z. Ding, “Sub-channel scheduling, task assignment, and power allocation for oma-based and noma-based mec systems,” *IEEE Trans. Commun.*, vol. PP, no. 99, pp. 1–1, 2020.
- [14] E. Zitzler and L. Thiele, “Multi-objective evolutionary algorithms: A comparative case study and the strength pareto approach,” *IEEE trans. Evolutionary Computation*, vol. 3, no. 4, pp. 257–271, 1999.
- [15] J. Schulman, F. Wolski, P. Dhariwal, A. Radford, and O. Klimov, “Proximal policy optimization algorithms,” *arXiv preprint arXiv:1707.06347*, 2017.
- [16] J. Schulman, P. Moritz, S. Levine, M. Jordan, and P. Abbeel, “High-dimensional continuous control using generalized advantage estimation,” *arXiv preprint arXiv:1506.02438*, 2015.
- [17] S. Parisi, M. Pirotta, N. Smacchia, L. Bascetta, and M. Restelli, “Policy gradient approaches for multi-objective sequential decision making,” in *2014 International Joint Conference on Neural Networks (IJCNN)*. IEEE, 2014, pp. 2323–2330.
- [18] K. He, X. Zhang, S. Ren, and J. Sun, “Deep residual learning for image recognition,” in *Proceedings of the IEEE conference on computer vision and pattern recognition*, 2016, pp. 770–778.
- [19] S. Natarajan and P. Tadepalli, “Dynamic preferences in multi-criteria reinforcement learning,” in *Proceedings of the 22nd International Conference on Machine Learning*, 2005, pp. 601–608.
- [20] “Ieee standard for telecommunications and information exchange between systems - lan/man specific requirements - part 11: Wireless medium access control (mac) and physical layer (phy) specifications: High speed physical layer in the 5 ghz band,” *IEEE Std 802.11a-1999*, pp. 1–102, 1999.
- [21] L. Li, W. Chu, J. Langford, and R. E. Schapire, “A contextual-bandit approach to personalized news article recommendation,” in *Proceedings of the 19th international conference on World wide web*, 2010, pp. 661–670.
- [22] L. Chen and J. Xu, “Task replication for vehicular cloud: Contextual combinatorial bandit with delayed feedback,” in *IEEE INFOCOM 2019-IEEE Conference on Computer Communications*. IEEE, 2019, pp. 748–756.
- [23] H. Zhao, X. Li, S. Han, L. Yan, and J. Yu, “Collaboration-aware relay selection for auv in internet of underwater network: Evolving contextual bandit learning approach,” *IEEE Internet of Things Journal*, 2022.
- [24] S. Bi and Y. J. Zhang, “Computation rate maximization for wireless powered mobile-edge computing with binary computation offloading,” *IEEE Transactions on Wireless Communications*, vol. 17, no. 6, pp. 4177–4190, 2018.
- [25] T. X. Tran and D. Pompili, “Joint task offloading and resource allocation for multi-server mobile-edge computing networks,” *IEEE Transactions on Vehicular Technology*, vol. 68, no. 1, pp. 856–868, 2018.